

# A Tool for Assessing the Consequences for Populations and Infrastructure resulting from an Asteroid Impact

Nicholas J. Bailey and Graham G. Swinerd

*School of Engineering Sciences, University of Southampton, Southampton, Hampshire, SO17 1BJ, UK*

*and*

Richard C. Crowther

*Space Engineering and Technology Division, Space Science and Technology Department,  
CCLRC Rutherford Appleton Laboratory, Chilton, Oxfordshire, OX11 0QX, UK*

**This paper concerns the development and application of a software tool, called NEOimpactor, for studying the human and economic consequences resulting from the impact of a sub-kilometer asteroid on the Earth. The modular software is developed using novel database architecture and utilizes impact process models available in the literature. The results contained within this paper are derived from a study performed to investigate which countries are at greatest risk from an impacting asteroid. A series of impacts are simulated uniformly across the globe with the human casualty figure and infrastructure damage estimates collated for each country. These are then used to rank the most strongly affected countries. Investigation is made of the effect of changing one characteristic of the impacting asteroid. These data provide insight into which countries face the greatest risk from an impact as well as those most vulnerable to the consequences of an impact.**

## Nomenclature

<i>NEA</i>	=	near earth asteroid
<i>NEO</i>	=	near earth object
<i>IGE</i>	=	impact generated effect

## I. Introduction

**B**Y its very nature, the threat to the Earth from an asteroid impact, in particular those classified as Near Earth Asteroids, is global. Present asteroid models tend to focus on a particular aspect of the impact process, from atmospheric entry to impact mechanics. The approach taken in this work was to draw from this large knowledge base of impact models to develop a global impact simulator, the focus of which is the consequences for human populations and the associated infrastructure damage. Recent hurricanes, for example Katrina<sup>1</sup> in 2005, and the Indian Ocean tsunami<sup>2-3</sup> have helped to highlight man's vulnerability to natural disasters and the subsequent hazards. However, the asteroid natural hazard remains perhaps the greatest threat to mankind.

The study detailed in this paper focuses on the development of a software tool, NEOimpactor, to quantify casualty and damage estimations following a NEO impact. There were a number of challenges to be overcome, notably the data handling requirement and the ability to manage the errors involved. In order to handle the large datasets, which contain information about the Earth, an internal database structure was developed to compile and store raw data and simulation results and to enable data retrieval.

Error is a continual problem with simulations involving asteroid impacts. Data such as a country's population, infrastructure and land area held within the database have compared favorably with real world data (two thirds of the countries data are within 10% of real world values). However, there is great difficulty in assessing the accuracy of a particular impact's casualty and damage figures due to the lack of real world data. Having no first hand empirical evidence from observed impacts, except the 1908 Tunguska event<sup>4</sup>, and no recorded evidence of any asteroid-induced fatalities, except some reports from China<sup>5</sup>, there exists no comparison to enable the errors to be defined. As

the data produced by any one single impact simulation is likely to have significant error bounds, the approach adopted in this study offers a novel means of producing workable data. Comparisons of multiple impact events to provide relative data eliminate the specific inaccuracies involved with a single event. This approach was implemented by repeatedly impacting the Earth with an impactor having the same characteristics into a predetermined grid array.

Such a multi-run global impact simulation was implemented to investigate the relative threat posed by an asteroid impact for each country in the world. By impacting a user-defined asteroid uniformly across the globe, the casualty and damage figures are recorded individually for each country worldwide. Once collated, the data can be manipulated to rank all countries in order of those most affected. Various attributes that alter this ranking are investigated with the results provided in a tabular form.

## II. Methodology

Studies of the literature revealed three research fields associated with an asteroid strike. The earliest work relates to the atmospheric passage of the body as it is captured by the Earth's gravitational field. Investigations stemmed from reports of the 1908 Tunguska event with the focus of modeling such an object to determine its characteristics, such as that by Chyba et al.<sup>6</sup>. In the NEOimpactor model atmospheric passage is tracked via a force propagator using a Runge Kutta integration algorithm to plot the asteroid path. The equations detailing the mass lost due to ablation and fragmentation have been derived from the work of Hills & Goda<sup>7</sup>. Fragmentation is accounted for within the NEOimpactor model, drawing on the work by Fritsche et al.<sup>8</sup>. However, this is disabled in the present study for simplicity.

At the point of impact, be it land or ocean, it is assumed that there is a complete transfer of the kinetic energy into the various impact generated effects (IGE's). Land impacts are characterized using the IGE models developed by Collins, Melosh & Marcus<sup>9</sup> for the Arizona web-based Impact Effects program. Four principal IGEs are modeled – the above ground pressure blast wave, thermal radiation from the expanding fireball, the ground transmitted seismic shock energy and the distribution of ejecta excavated from the impact site. These four effects are simulated simultaneously by the system and provide the basis for analyzing the consequences for humans and infrastructure from land impacts.

Ocean impacts are characterized by the generation of a tsunami wave which propagates from the impact site to coastlines around the globe. Cavitation of the ocean at the point of impact and successive tsunami generation has been modeled by Ward & Asphaug<sup>10</sup>. These models have been implemented into NEOimpactor together with an ocean 'neural network' style path determination which simulates the wave's ability to diffract around coastlines. The consequences of the incident tsunami wave upon the coastlines affected are calculated from the shoaling characteristics of the wave, namely the run-up and run-in distances.

### A. NEOimpactor Software Development

A modular programming approach was chosen for the software architecture to enable future improvements and features to be incorporated smoothly. Each of the three phases mentioned previously were developed as an independent module. In order to utilize the information generated by these modules, in particular the land and ocean IGE distributions, a core module was constructed to handle the impact phase modules as well as the human-computer interface. This interface was built using the Microsoft Visual Studio environment. The architecture of this core module has been based on a database model which offers a solution to the handling requirement and manipulation of large datasets. Three 'layer' types are contained within the database: raw dataset layers, IGE layers and interaction layers. Each layer contains data across the entire globe, which was divided into a series of cells of equal latitude and longitude bins. The database maintains the data in a spherical system to avoid the errors inherent in any cartographic projection and can be pictured as spherical overlays on a cellular globe. Calculations are also performed using the spherical coordinate system to account for the nearly spherical Earth. Thus, any cell on the globe can be quickly sampled across all layers to retrieve its characteristics.

Of particular importance are the population and infrastructure layers, derived from datasets available on the internet. The population data was sourced from the Socioeconomic Data and Applications Center<sup>i</sup>. The population of each cell is derived from the summation of the population density multiplied by the area of each cell. The global population (sourced from the CIA World Factbook<sup>ii</sup>) is divided by this value to derive a density multiplier. Multiplying the cell area, density level and multiplier provides a total area-corrected population figure for each cell.

---

<sup>i</sup> Socioeconomic Data and Applications Center [online] <<http://sedac.ciesin.columbia.edu/gpw/>>

<sup>ii</sup> CIA World Factbook [online] <<https://www.cia.gov/cia/publications/factbook>>

As no global infrastructure dataset was available, an approximation was made by using a grayscale nighttime light pollution world map and making the assumption that regions of greater light pollution correlated to higher infrastructure density. Using a value for the global economic value<sup>11</sup> the infrastructure value for each cell was inferred using a similar method to the population density.

At the point where the asteroid reaches the ground one of two impact phase modules were called, one for ocean impacts and the other for land impacts. Both modules combine the asteroid's characteristics (such as mass, velocity and density) with information from the database regarding the impact site (e.g. the elevation or depth, ground type and country) to determine the IGEs produced. These effect distributions are stored within database layers. Following impact, the core program module performs interactions between the IGE layers and the dataset layers to calculate the percentage of inhabitants and infrastructure in each cell that would be affected. This percentage multiplied by the cell population and infrastructure values provide the casualty and damage layer data, stored again within the database. From this point information can be extracted from the database by cross referencing layers to derive unique raw data or produce bitmap maps (formatted in a Plate Carrée cylindrical projection).

### B. Case Study Methodology

In order to study the global threat of an asteroid impact, the software was used to handle multiple impact events and provide a correlation of results. To achieve this, a sub program was constructed within NEOimpactor which performed a succession of impact events as described above. For simplicity, the globe was divided into a uniform grid of latitude and longitude bins, into which an asteroid was impacted. The casualty and damage figures for each grid cell impact are recorded in an external data file for future manipulation.

Casualty and damage values for each cell impact can then be processed into a bitmap map file. This process takes the maximum and minimum casualty and damage figures across the grid and equalizes the grey-scale bitmap shading according to these limits, with the darkest cells representing the strongest impact consequences. These bitmaps, for example Fig. 1, provide a useful method of depicting the relative consequences for individual real impacts. However, the raw data for each impact can be further analyzed to discover the consequences for each country affected by any of the grid impacts.

When considering the scenario of an impacting asteroid, there are a number of principal variables to be defined, each of which have an effect on the body's energy. Size, mass and velocity contribute predominantly to the kinetic energy reaching the surface, while the incoming trajectory will alter the atmospheric ablation and breakup characteristics. In this study the trajectory was aligned to the vertical for each cell impact and the fragmentation model was disabled to keep uniformity across the grid. The typical asteroid used for the simulation is a 500 m in diameter, spherical body composed of a soft stone material ( $1500 \text{ kg/m}^3$ ) traveling at 12000 m/s. Such an asteroid delivers  $1.07 \times 10^{18}$  joules of kinetic energy at the point of impact following atmospheric entry. While the global grid system enables each impact to be compared with one another, thus developing the relative consequences of one impact compared to another, different diameter objects were simulated to provide a comparison with the default. Impactor diameter was chosen as the parameter to alter due to its large influence on the body's characteristics.

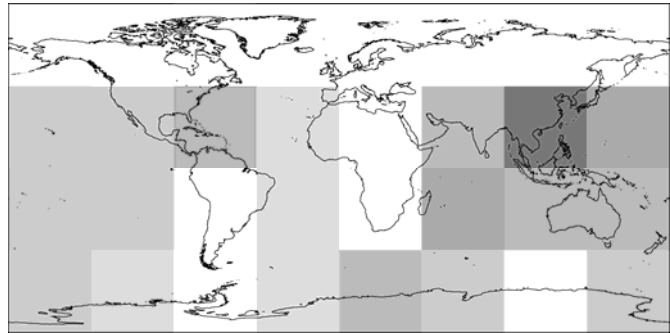


**Figure 1. Map of grid impact simulation with dark shading denoting large casualty figures.**

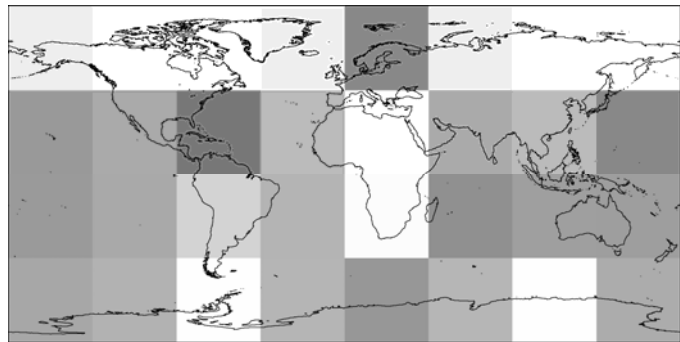


**Figure 2. Map of grid impact simulation with dark shading denoting high infrastructure damage.**

### III. Results

#### A. Global Casualty and Damage Maps

An eight by four (32 cell) grid was chosen to optimize processing time, though higher resolution grids are possible with the NEOimpactor system. Figure 1 presents the casualty data resulting from an impact of the asteroid defined above into the center of each cell. The casualty figures used for the shading are a summation of all the casualties in all countries of the world. It is clear to see from this image that ocean impacts present the most significant risk for this 500 m diameter object, in particular those impacting around southeast Asia and Central America. Indeed the cell covering southeast China and the Philippines generated the largest death toll which was expected due to the very high population density in this region of the world. While impacts into the central ocean regions still present a significant threat to coastal populations, the attenuation of the tsunami as it spreads acts to dissipate the energy and reduce the damage potential of the shoaling wave. Indeed, the darker cell centered on the Caribbean demonstrates that ocean impacts in proximity to land, especially heavily populated coastal regions, will result in significantly higher casualty figures.

The relatively low overall population density of inland Central Africa, Russia, Canada and South America result in the impacts occurring here generating relatively few casualties. However, it is important to stress that these results do not suggest that no casualties are generated by land-striking asteroids. Compared to the destructive potential and far reaching capabilities of a tsunami wave, the land-impact events recorded produce significantly fewer casualties. Thus the greatest overall risk to humanity resulting from a 500 m asteroid would be from an ocean impact event. The second limiting factor in land impacts is their high dependence on location. While two ocean impacts 20 km apart may generate only negligibly different consequences, on land such a separation could mean the difference between a direct strike on a city and an unpopulated area. A higher resolution grid will generate more land impacts and locate regions which present a significant land impact risk.

Infrastructure damage values are depicted in Fig. 2 using the same procedure as was used to generate casualty figures. Here we see a similar picture, with ocean impact cells accounting for the largest infrastructure damage figures due to the destructive reach of the propagating tsunami wave. The Caribbean is again highlighted as having a significant impact risk due to the number of countries and especially the large number of capital cities located close to or on the coast. However, around Southeast Asia and Australasia, the greatest tsunami threat has been shifted south so that impacts east and west of Australia are producing greater infrastructure destruction. Australia is particularly prone to tsunami damage in economic terms due to the positioning of its major cities on the coast.



Figure 3. Casualty map for 100 m diameter asteroid.

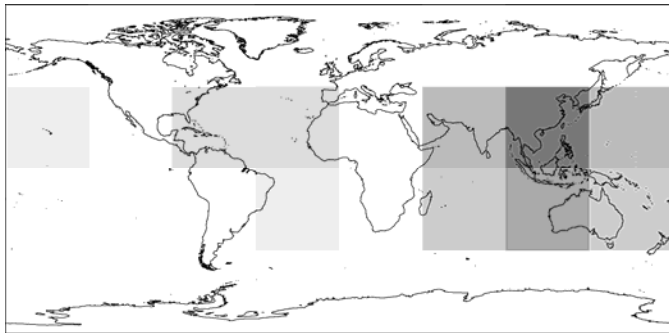


Figure 4. Casualty map for 200 m diameter asteroid.

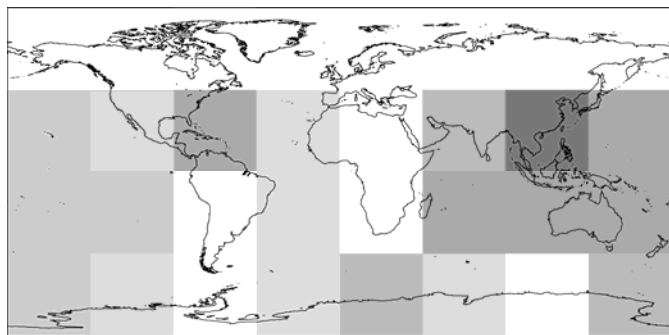
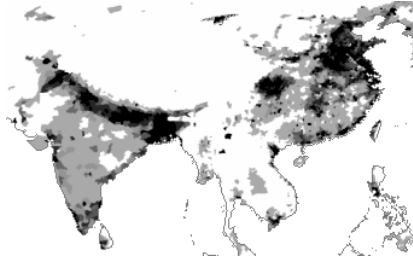


Figure 5. Casualty map for 1000 m diameter asteroid.



**Figure 6. Population density across southeast Asia.**

While impact around India and China will result in significant casualty figures due to the high population densities, the local supporting infrastructure is far less developed than regions such as Europe, meaning the relative damage figure is reduced. The most notable distinction between the casualty and damage distributions is the generation of significant infrastructure damage in Northern Europe, in particular, Scandinavia. This traditionally ‘developed’ region has in place significant physical infrastructure, from communication and transportation networks to industrial zones and substantial urban conurbations. In the night-time light pollution data, used to develop the density dataset for global infrastructure, Europe appears as a strong source indicating a large region of developed infrastructure. The overall threat to Europe’s infrastructure resulting from a land impact is further highlighted in the following section.

**B. Variation in Asteroid Diameter**

Varying the impactor diameter provides further insight into the threat faced by the global community. At small diameters (those which just begin to survive the atmospheric entry phase intact) the IGEs generated are naturally weaker. Ocean impact tsunamis become weak to the point that only those within close proximity of the shoreline can generate any significant casualties or damage. Therefore the area of the globe for which tsunamis are the dominant IGE reduces to a thin strip surrounding all coastlines. An impact into such a region would generate a high level of destruction, but the probability of such an impact is very low. Instead, the consequences for a land impact become more significant.

The precise dependence on impact site location as mentioned previously will change very little with different diameter impactors as the land area itself does not change. Thus as this strip of tsunami dominance reduces the land impact hazard becomes dominant. Figure 3 demonstrates this effect with strong casualty figure signals on land very close to the coastline. As the object size is increased, Fig. 4, ocean impacts become more significant. It would appear from these results that a threshold diameter for the transition of impact severity from land impact to ocean impact occurs in the range 100 m to 200 m.

**C. Country Listing**

*1. Raw Percentage of Total*

Raw data detailing the number of casualties and the damage for each country of the Earth for every grid-cell impact was generated by NEOimpactor and stored as a data file. These data were manipulated to sum the total casualty and damage figures for each country over the entire grid. When ordered, this generates a list of which countries have been affected most severely by the uniform distribution of impacts (or average impact). Normalizing these figures by the total global casualty and damage figures provided the country’s casualty and damage rates as a percentage of the total global figure. Table 1 and 2 present the top ten countries within these two listings using the standard 500 m diameter asteroid as defined above.

Studying the casualty ranking in Table 1 shows that these country’s casualties account for 66% of the global casualties produced and contain some of the largest coastal cities in the world, including Tokyo, New York, Shanghai, Jakarta and

**Table 1. Percentage of global impact casualties.**

	% of Global Casualty	% Summation
China	17.69	17.7
Indonesia	10.03	27.7
India	8.32	36.0
Japan	7.19	43.2
United States	6.31	49.5
Philippines	4.32	53.9
Italy	3.77	57.6
United Kingdom	3.28	60.9
Brazil	2.66	63.6
Nigeria	2.39	66.0

**Table 2. Percentage of global infrastructure damage.**

	% of Global Damage	% Summation
United States	9.85	9.9
China	7.69	17.5
Sweden	5.22	22.8
Canada	5.10	27.9
Japan	4.20	32.1
Mexico	4.18	36.2
Brazil	3.29	39.5
United Kingdom	3.24	42.8
Norway	3.09	45.8
Russia	3.07	48.9

Rio de Janeiro. The ranking based on infrastructure damage accounts for just below 50% of the total damage sustained over the 250 countries in the database. China, Japan, the United States, the United Kingdom and Brazil appear in both lists and are therefore potentially face a larger risk to their population and economy.

The heightened vulnerability of all top ten countries stems from two factors, namely the country's total population or infrastructure wealth and the total land area. Of the fifteen countries which appear, eight occur in the top ten highest populations, six in the top ten by total infrastructure value, and six in the top ten countries by land area. Significantly none of the countries listed are land-locked and each possess a significant length of coastline in proportion to their area, with Nigeria being the exception. As demonstrated previously, any coastline is vulnerable to the tsunamis generated by a wide range of ocean impact locations and it is predominantly in these locations that the casualty and damage totals are mostly increased. In general, countries with larger land area also have a greater chance of receiving a direct land impact. Unsurprisingly four of the countries listed are island nations, and by their very nature will have a large ratio of coastline to land area, and as such are at a higher risk.

China's risk is predominantly associated with its densely populated southwestern coastline, a product of the wealth associated with maritime trade and fishing, as well as the large populations living in and around the capital Beijing - see Fig 6. Having the largest population of any country automatically places more people at risk and the vulnerability to Pacific impact generated tsunamis make the mitigation task challenging.

The United States bears a significant risk due to its exposure to the two largest oceans and the possibility of NEOs impacting them. Again there are a number of large cities on these shores which face an immediate threat from tsunami inundation. The experience of recent severe hurricane events such as Katrina has stimulated research into the mitigation of the risk posed by natural hazards and their effects. Such meteorological hazards are, however, small in comparison to the potential devastation from even a modest sized asteroid.

The appearance of the UK in both lists should be considered. Out of the countries present in both lists, it has the smallest population (below half that of Japan, the second smallest) and so would not naturally be expected to be at such a great risk on a global scale. However, being an island nation with a comparatively small area to receive a land impact heightens the risk from ocean impact generated tsunamis. The presence of a number of large cities along the south and western coastlines places many people and much infrastructure at risk. Such a large risk for a reasonably small country demands that the threat be taken seriously, and considering the relative lack of risk from other natural disasters such as volcanoes, earthquakes and hurricanes, the asteroid hazard is perhaps the greatest threat.

## 2. Land Area Corrected Casualty Listing

Division of each country's total casualty figure by the land area for that country and converting to a percentage generates an area-corrected casualty density list. The top ten are listed in Table 3. Of these ten, nine are island nations and five are found within the Caribbean. Considering the previous results in Fig. 1, which highlighted Central America as location which induces large casualty figures, the high listing of these nations is confirmed. Being such small islands the potential for populations to live away from the coast, and indeed not be dependent on it, is very small, and so they are immediately at risk from tsunami inundation. What this rating seeks to highlight is countries that, in the event of an impact, have little means of escape. The casualty density estimates reflect how densely populated the country is and the potential for the population to

**Table 3. Country area corrected casualty density.**

	Area, km <sup>2</sup>	% Casualty Density
Puerto Rico	10,281	12.70
Haiti	26,558	7.16
Jamaica	11,050	7.01
Singapore	401	5.39
Trinidad and Tobago	4,731	5.35
Reunion	1,870	5.29
El Salvador	21,815	5.22
S. Georgia Islands	3,507	3.80
Guam	1,170	2.67
Guadeloupe	1,925	2.67

**Table 4. Percentage of country population lost.**

	Population	% Lost
S. Georgia Islands	333,650	1.46
Guinea Bissau	227,444	1.28
French Southern & Antarctic Lands	500,529	1.07
Jan Mayen	1,803	1.04
Virgin Islands	38,671	1.01
Solomon Islands	133,091	0.99
Panama	1,850,760	0.99
Samoa	14,339	0.92
Jamaica	3,259,120	0.87
Puerto Rico	5,671,940	0.84

evacuate.

This highlights the level of error indicative in the code. When impacting a large country covering many cells in the database, the number of IGE it is affected by will help to smooth out the noise error associated with different individual impacts. However, with small island nations, each IGE will affect all areas of the island nearly uniformly, and so any error noise in the calculations will not be smoothed.

### *3. Percentage Population Lost*

The third ranking, shown in Table 4, gives the percentage of a country's population lost due to the averaged impact. Small island nations make up all but one (Panama) of the top ranked countries. The maximum loss of 1.46% of the population of the South Georgia Islands does not represent any single impact in the grid but rather the average of all the impacts performed.

The use of this data is in identifying which populations are almost completely threatened by the asteroid natural hazard. For example, while an impact into the United States may kill more people the chance of wiping out the entire cultural and social heritage is slim. However, the island nations identified could potentially be entirely devastated resulting in a loss to society of more than simply a population. Such communities at risk from total annihilation might require particular protection by the international community.

## **IV. Conclusion**

The NEOimpactor software tool provides a platform which to investigate the NEO hazard on a global scale. Implementation of the database architectural design model enables multiple investigations to be performed using one basic simulation method. In this paper the global grid methodology is successfully used to study the global hazard as well as an individual country's cumulative risk. Identification of a transition diameter at which the most significant impact severity progressed from land to ocean impacts provides the basis of a threshold diameter for decision making. Below such a threshold where ocean impacts are unlikely to cause much significant damage, the risk posed is predominantly to a single country (or possible bordering countries if the impact site lies near to a political border), and while any impact would be of global significance, the consequences are localized. As the diameter surpasses this threshold, and the probability exists for an ocean impact, the event becomes of international importance due to the potential number of countries that would be affected by a single event. The decision making processes involved aim to specifically define at what diameter an Earth crossing asteroid becomes a focus for proactive multi-lateral cooperation in terms of impact mitigation. Increasingly fine resolution multi-impact simulations will seek to define this threshold more accurately. Performing parametric studies on each of the asteroid characteristics will identify which are most critical to the threshold sensitivity.

The importance of the country ranking investigations lies in the identification of who and what is most at risk from the global hazard. While the probability of an asteroid impacting the Earth is remote, and NEO surveys such as Catalina<sup>11</sup> and Spaceguard<sup>12</sup> seek to catalogue the unknown population. The possibility of an impact, in particular from a small sub-kilometer body, still exists. Therefore identification of the regions most at risk will help aid the international community in its development of strategies to minimize this risk. Highlighting the principal countries which face the largest risk offers some suggestion as to which countries need to work together to help mitigate the threat (and indeed the United States is actively involved in such activities as they have most to lose). Furthermore, data such as the area corrected list, Table 3, offers feedback on those countries that, while not suffering the same great losses, are vulnerable because of having no effective evacuation options. This will result in post-impact complications for refugees, or a significant risk of loss of an entire society and heritage. Future work using NEOimpactor will seek to improve the database model and IGE models. Simulations utilizing and cross referencing different layers of the database will continue to be performed to study the global and regional effects of asteroid impacts.

## **Acknowledgments**

N.J. Bailey would like to acknowledge the support and encouragement of his colleagues and especially thanks Dr Hugh Lewis for his technical advice and supervision. The authors would also like to recognize the financial of the British National Space Center.

## **References**

<sup>1</sup>Graettinger, Andrew J.; Van De Lindt, John W.; Gupta, Rakesh; Pryor, Steven E.; Skaggs, Thomas D.; Fridley, Kenneth J., "Overview of Wind Damage to Woodframe Structure Caused by Hurricane Katrina", Structures Congress 2006: Structural

Engineering and Public Safety, Vol. 2006, American Society of Civil Engineers, Reston, VA 20191-4400, United States, 2006, pp. 57

<sup>2</sup>Ghobarah, A., Saatcioglu, M., Nistor, I., “The Impact of the 26 December 2004 Earthquake and Tsunami on Structures and Infrastructure”, *Engineering Structures*, Vol. 28, No. 2, 2006, pp. 312-326.

<sup>3</sup>Lay, T., Kanamori, H., Ammon, C.J., Nettles, M., Ward, S.N., Aster, R.C. et al., “The Great Sumatra-Andaman Earthquake of 26 December 2004”, *Science*, Vol. 308, No. 5725, 2005, pp. 1127-1133.

<sup>4</sup>Bronshten, V.A., “Nature and Destruction of the Tunguska Cosmical Body”, *Planetary and Space Science*, Vol. 48, No. 9, 2000, pp. 855-870.

<sup>5</sup>Yau, K., Weissman, P., Yeomans, D., “Meteorite Falls in China and some Related Human Casualty Events”, Vol. 29, No. 6, 1994, pp. 864-871.

<sup>6</sup>Chyba, C.F., Thomas, P.J., Zahnle, K.J., “The 1908 Tunguska Explosion. Atmospheric Disruption of a Stony Asteroid”, *Nature*, Vol. 361, No. 6407, 1993, pp. 40-44.

<sup>7</sup>Hills, J.G., Goda, M.P., “The Fragmentation of Small Asteroids in the Atmosphere”, *Astronomical Journal*, Vol. 105, No.3, 1993, pp. 1114-1144.

<sup>8</sup>Fritsche, B., Klinkrad, H., Kashkovsky, A., Grinberg, E., “Spacecraft Disintegration During Uncontrolled Atmospheric Re-entry”, *Acta Astronautica*, Vol. 47, No. 2, 2000, pp. 513-522.

<sup>9</sup>Collins, G.S., Melosh, H.J., Marcus, R.A., “Earth Impact Effects Program: a Web-based Computer Program for Calculating the Regional Environmental Consequences of a Meteoroid Impact on Earth”, *Meteoritics & Planetary Science*, Vol. 40, No. 6, 2005, pp. 817-840.

<sup>10</sup>Ward, S.N., Asphaug, E., “Asteroid Impact Tsunami: a Probabilistic Hazard Assessment”, *Icarus*, Vol. 145, No. 1, 2000, pp. 64-78.

<sup>11</sup>Jedicke, R., Morbidelli, A., Spahr, T., Petit, J.-M., Bottke, W.F., Jr., “Earth and Space-based NEO Survey Simulations: Prospects for Achieving the Spaceguard Goal”, *Icarus*, Vol. 161, No. 1, 2003, pp. 17-33.

<sup>12</sup>Stokes, G. H., Yeomans, D. K., Bottke, W. F., Chesley, S. R., Evans, J. B., Gold, R. E., “Study to Determine the Feasibility of Extending the Search for Near-Earth Objects to Smaller Limiting Diameters”, Report of the Near-Earth Object Science Definition Team, URL: <http://neo.jpl.nasa.gov/neo/neoreport030825.pdf>[cited 15 February 2007].